Progress In Electromagnetics Research Letters, Vol. 92, 69–74, 2020

Compact SICC Dual-Band and UWB Filters Using Multimode Technology

Xiu-Guang Chen, Guo Hui Li*, Zhi-Wei Shi, and Shuo-Dan Feng

Abstract—In this paper, a dual-band bandpass filter using sixteenth-mode substrate integrated circular cavity (SM-SICC) and a novel ultra-wideband (UWB) bandpass filter (BPF) using eighth-mode SICC (EM-SICC) cavity are presented. The TM101, TM102, and TM201 resonant modes of the substrate integrated waveguide (SIW) circular cavity are used to design the dual-band filter, where the resonant frequencies can be shifted to the desired frequency through adjusting the position and size of complementary split-ring resonator (CSRR). In addition, the TM101, TM102, TM103, and TM104 resonant modes are employed to realize the UWB filter. A transmission zero appears by introducing the CSRR in the middle of the SICC, so the dual-band BPF and UWB BPF with high selectivity are realized. The proposed filters possess compact size, because of the EM-SICC and SM-SICC. The dual-band filter operating at 7.79 and 12.83 GHz is fabricated in SM-SICC with 3-dB fractional bandwidths (FBWs) of 7.8% and 31.25%, respectively. The UWB filter with FBW of 97% is simulated in EM-SICC. Compact circuit sizes and excellent measured performances have been achieved for the two filters.

1. INTRODUCTION

The ever-accelerated modern multi-standard communication system requires advanced microwave components, especially filters to have high-performance and compact-size [1]. Recently, multi-mode filters have received significant research attention for their attractive characteristics such as few resonating elements, good passband selectivity and advanced asymmetrical elliptic or quasi-elliptic response [2]. To date, various types of dual-band and UWB bandpass filters have been proposed using multimode approach. In [3], resonators based on SICC structure are discussed. A planar BPF based on SICC resonator is presented, but it is not suitable to be integrated into multilayer circuit modules due to its large volume. BPFs based on SIW in low temperature co-fired ceramic (LTCC) have small size and excellent performance, but their structures are complicated and require high fabrication precision. However, in some cases, the multimode approach can be used to design dual-band filters with only a single SIW cavity.

This paper presents a dual-band bandpass filter using SM-SICC and a novel UWB bandpass filter using EM-SICC cavity. Compared to the conventional SIW cavity, the size of the SM-SICC cavity is reduced to a factor of 1/16 while maintaining the same resonant frequency.

2. ANALYSIS AND DESIGN OF COMPACT SICC DUAL-BAND AND UWB FILTERS

In this paper, the EM-SICC and SM-SICC structures are used to realize a UWB filter and a compact dual-band filter operating at 7.79 and 12.83 GHz. EM-SICC and SM-SICC are realized by dividing the

Received 19 March 2020, Accepted 4 June 2020, Scheduled 22 June 2020
* Corresponding author: Guo Hui Li (shghlee@163.com).
The authors are with the Key Laboratory of Specialty Fiber Optics and Optical Access Network, Shanghai University, Shanghai 200072, China.

complete substrate into round cavity by 1/8 and 1/16, respectively. It is implemented on a Rogers 5880 substrate with dielectric permittivity $\varepsilon_r = 2.2$, substrate thickness $h = 0.787\,\mathrm{mm}$, and $\tan\delta = 0.0009$. The simulations are performed on Ansys Electromagnetics HFSS 15.0, while the measurements are executed by the Agilent N5227A vector network analyzer.

The geometry of the SICC resonator is shown in Fig. 1(a). It consists of the top and bottom metal layers, which are connected with metal via arrays. The radius R of the SICC can be determined by theories of solid wall circular cavity and guidelines in [4]. Fig. 1(b) depicts the simulated E fields in the perturbed cavity at the resonant frequencies of the first four modes in the proposed cavity.

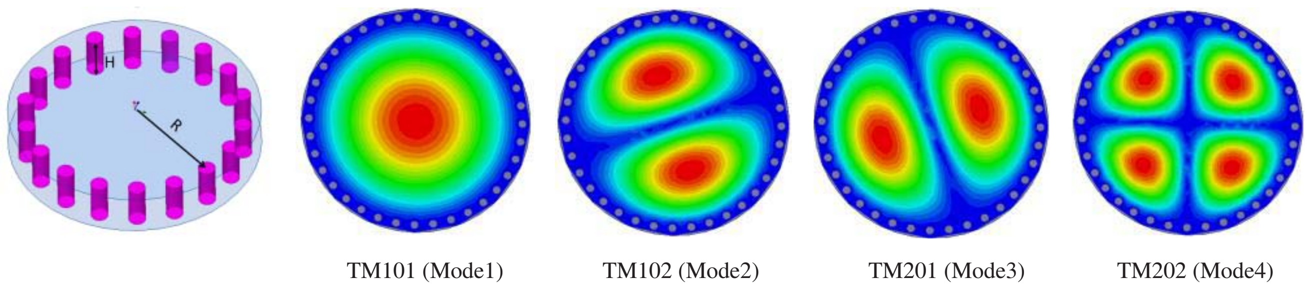

(a) (b)

Figure 1. (a) Configuration of the SICC cavity. (b) Simulated E-fields of the first four resonant modes in the proposed cavity.

The resonant frequency of the empty circular cavities (without perturbation) can be determined by Eq. (1) as suggested in [5]

$$f_{mnl} = \begin{cases} \dfrac{c}{2\pi\sqrt{\mu_r\varepsilon_r}}\sqrt{\left(\dfrac{p'_{mn}}{R}\right)^2 + \left(\dfrac{l\pi}{z}\right)^2} & \mathrm{TE}_{mnl}\ \text{mode} \\ \dfrac{c}{2\pi\sqrt{\mu_r\varepsilon_r}}\sqrt{\left(\dfrac{p_{mn}}{R}\right)^2 + \left(\dfrac{l\pi}{z}\right)^2} & \mathrm{TM}_{mnl}\ \text{mode} \end{cases} \tag{1}$$

where p'_{mn} and p_{mn} are the nth root of the mth Bessel function of the first order and its derivative respectively; c is the speed of light in free-space; ε_r and μ_r are relative permittivity and permeability; and R is the radius of SICC. Unlike the rectangular resonator, the directional current component of the mode in the circular cavity cannot be conducted, and only TM modes exist.

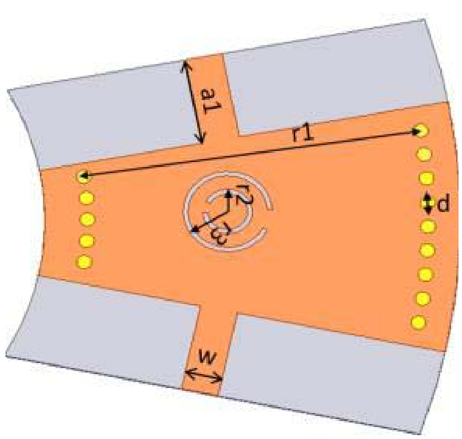

Figure 2. Configuration of the proposed dual-band filter.

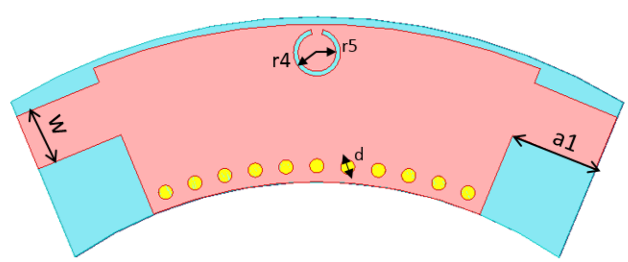

Figure 3. Configuration of the proposed UWB filter.

The configuration of the proposed filter I is shown in Fig. 2, where a CSRR is etched on the cavity. Two 50 Ω microstrip lines through a pair of coplanar waveguides are adopted as input/output ports. A novel UWB BPF (filter II) using eighth-mode substrate integrated waveguide (EMSIW) cavity is also shown in Fig. 3. In order to obtain the expected performance, all the parameters in Fig. 2 and Fig. 3 are optimized using full-wave EM simulator software (ANSYS HFSS 15.0). The final optimized parameters of the filters are: $a1 = 3.78$ mm, $r1 = 13.7$ mm, $d = 0.6$ mm, $r2 = 1$ mm, $r3 = 1.8$ mm, $w = 2.4$ mm, $r4 = 1$ mm, $r5 = 0.95$ mm.

The electric field distributions of the dominant mode and two degenerated modes in sixteenth-mode substrate integrated waveguide (SMSIW) cavity are shown in Fig. 4(a), Fig. 4(b), and Fig. 4(c), respectively, while the EMSIW cavity electric field distributions of the first three resonant modes are shown in Fig. 5(a), Fig. 5(b), and Fig. 5(c), using the full-wave eigenmode analysis. In Fig. 4, the CSRR arranged in a circle ring can bring the most distinct change for mode 1, while modes 2 and 3 are slightly perturbed. By shifting mode 3 toward mode 2, two passbands are generated, and the dual-band filter can be designed.

Figure 6 shows the coupling scheme of the proposed dual-band filter, where S and L in this scheme represent the source and load. For simplicity, only three couplings are considered by ignoring the minor couplings, for example: coupling between TM201 mode and TM102 mode. As shown in Fig. 6, three

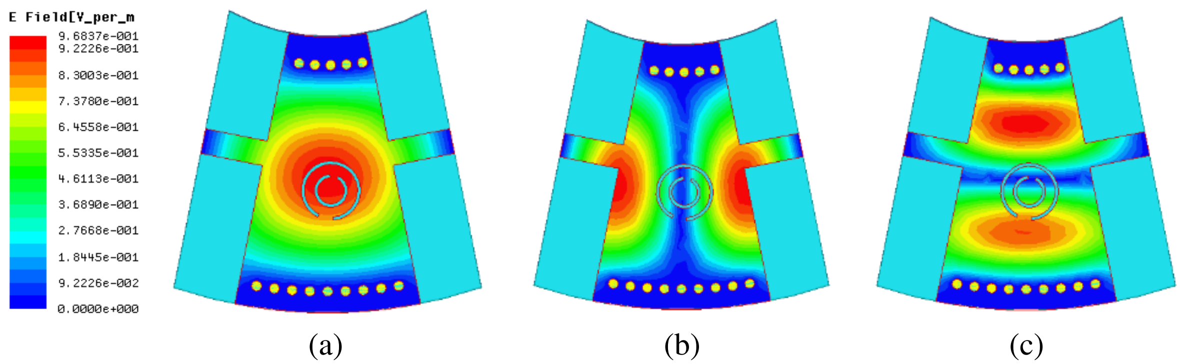

Figure 4. Simulated E-fields of the first three resonant modes in the proposed SMSIW cavity. (a) TM101 (Mode1), (b) TM102 (Mode2), (c) TM201 (Mode3).

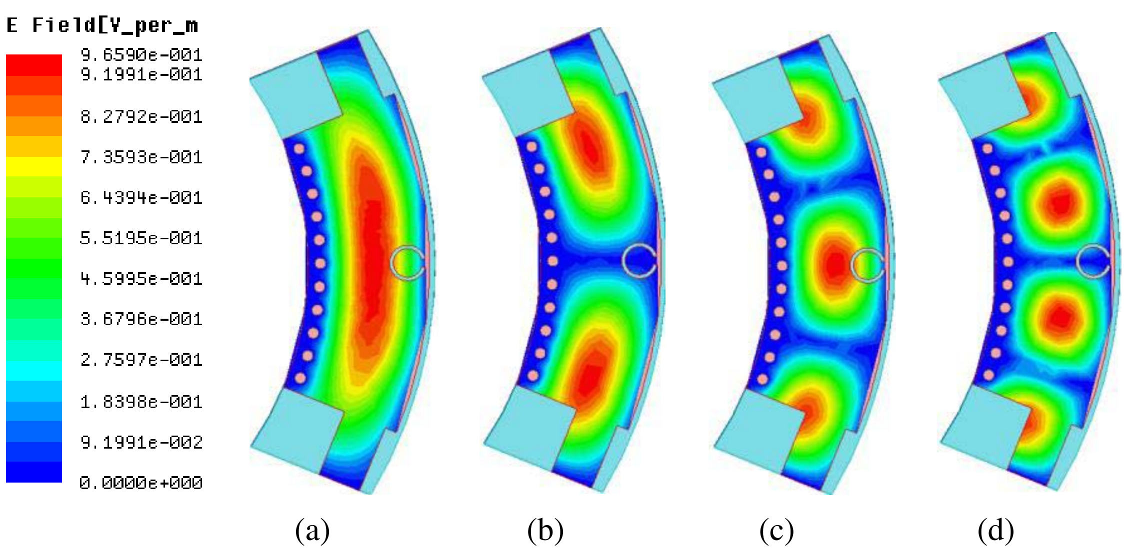

Figure 5. Simulated E-fields of the first four resonant modes in the proposed EMSIW cavity. (a) TM101, (b) TM102, (c) TM103, (d) TM104.

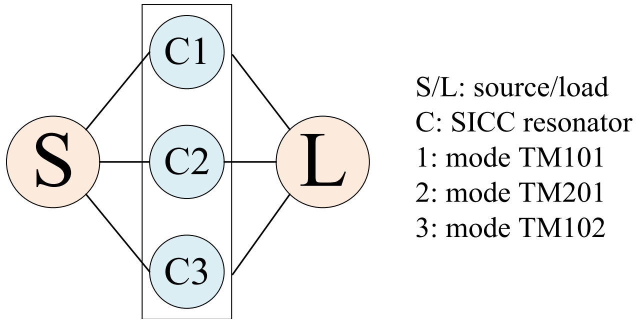

Figure 6. Coupling scheme of the dual-band filter.

separated paths from source to load are provided. These three paths correspond to the three modes of the bandpass filter.

The design and optimization procedures of the dimensions of the proposed filters can be summarized as follows.

1) Determine the initial size of the cavity according to the center frequency of the passbands.

2) Derive the design parameters, such as Q_e and M_{ij} from the prescribed specifications including the topologies, center frequencies (CFs), and the bandwidths of passbands using the synthesis procedures.

3) Determine the coupling parameters of the external I/O port and internal coupling structure by adjusting the position and size of the excitation port to load, the perturbation structure, offset and size of the coupling window relative to the center.

3. FABRICATION AND MEASUREMENT

In order to verify the feasibility of the above analysis, a dual-band filter using SM-SICC and a novel UWB filter using EM-SICC are fabricated. The simulation and measurement results are depicted in Fig. 7. As we can see from Fig. 7(a), for dual-band filter, the simulated CFs and 3-dB FBWs are 7.79 GHz and 12.83 GHz, 7.8% and 31.25%. The minimum in-band insertion loss is nearly 1.8 dB, and passband return loss is better than 18 dB. It is also found that one transmission zero is located at

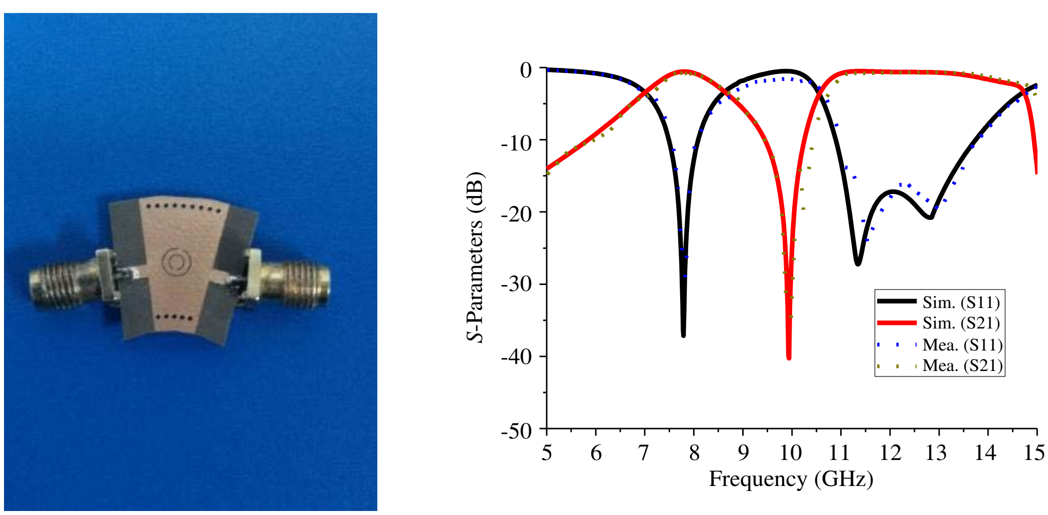

(a) (b)

Figure 7. Photograph and comparison of the simulated and the measured results of the dual-band bandpass filter. (a) Photograph. (b) $|S_{11}|$ and $|S_{21}|$.

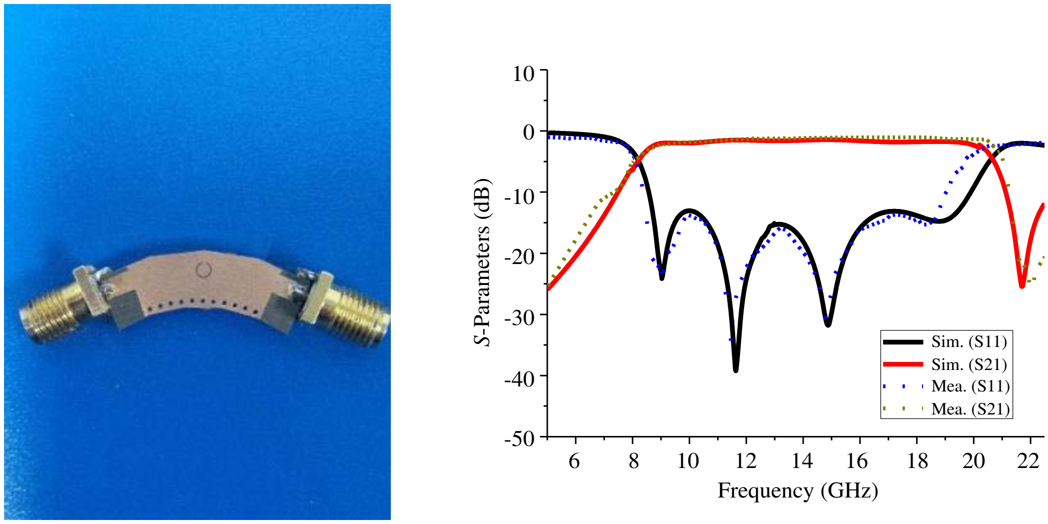

(a) (b)

Figure 8. Photograph and comparison of the simulated and the measured results of the UWB bandpass filter. (a) Photograph. (b) $|S_{11}|$ and $|S_{21}|$.

Table 1. Comparison between the proposed filters and the references.

		Size (λ_g)	IL (dB)	3 dB FBW (%)	Notch frequency (GHz)
[6]		2.97×1.45	< 1.18	28	No
[7]		0.87×0.66	< 1.77	113.0	5.8
[8]		2.2×0.85	< 2.1	79	No
[9]		0.9×0.9	< 0.95	25.43	No
[10]		0.9×0.22	< 3.7	120	4.08/6.57/8.96
This work	Dual-band filter	0.59×0.48	< 1.8	72	9.94
	UWB filter	0.67×0.21	< 1.6	97	No

9.94 GHz above the passband. Further work supports the view that the location of the transmission zero and CFs can be controlled by changing the dimension of the CSRR.

As shown in Fig. 8, the 3-dB FBW of UWB filter is 97%. It can be seen that the simulated passband return losses are above 12 dB. Only two cavities are needed in the proposed EM-SICC and SM-SICC filters, leading to more compact structures. The total dimensions of the filters are $22.6\,\text{mm} * 18.8\,\text{mm} * 0.787\,\text{mm}$, $26\,\text{mm} * 8\,\text{mm} * 0.787\,\text{mm}$, respectively. As can be seen from Table 1, the proposed BPFs achieve miniaturization and better bandwidth performance from the comparison of size and 3 dB FBW. The proposed dual-band filter achieves a larger bandwidth than those in [6, 9, 10], while keeping merits of low-insertion loss and compact circuit size. At the same time, the center frequency of passband can be adjusted by changing the position of CSSR, and one transmission zero is generated in the stopband. In addition, a new transmission zero is obtained by introducing the source load coupling, which further improves the frequency selectivity of the filter. Meanwhile, compared with [7, 8], the proposed UWB filter achieves more compact circuit size with almost relative bandwidth.

4. CONCLUSION

In this paper, based on the mode-shifting technique and CSRR, two novel filters using EM-SICC and SM-SICC are presented, where two passbands of the dual-band filter are centered at 7.79 and 12.83 GHz, respectively. The filters achieve good insertion loss and miniaturization. The simulated results show the validity and efficiency of the proposed method. The filters have compact size, simple configuration, low loss, and ease of fabrication, which make them suitable candidates for application in microwave communication systems. In order to validate the simulation results, compact SICC dual-band and UWB bandpass filters prototypes have been fabricated with standard PCB technology. The measured results are found to agree well with the simulated ones, demonstrating the feasibility of the proposed design method.

REFERENCES

1. Jia, D.-H., J. Deng, Y. Zhao, and K. Wu, "Quad-band multilayer SIW filter with high selectivity and controllable bandwidths," *Progress In Electromagnetics Research Letters*, Vol. 83, 133–138, 2019.
2. Li, J., S. S. Huang, H. Wang, and J. Z. Zhao, "A novel compact dual-wideband bandpass filter with multi-mode resonators," *Progress In Electromagnetics Research Letters*, Vol. 51, 79–85, 2015.
3. Azad, A. R. and A. Mohan, "A compact sixteenthmode substrate integrated waveguide bandpass filter with improved out-of-band performance," *Microwave and Optical Technology Letters*, Vol. 59, No. 7, 1728–1733, 2017.
4. Potelon, B., J. Bohorquez, J. Favennec, et al., "Design of Ku-band filter based on substrate-integrated circular cavities (SICCs)," *2006 IEEE MTT-S International Microwave Symposium Digest*, 1237–1240, IEEE, 2006.
5. Yang, Y.-N., G. H. Li, L. Sun, W. Yang, and X. Yang, "Design of compact bandpass filters using sixteenth mode and thirty-second mode SIW cavities," *Progress In Electromagnetics Research Letters*, Vol. 75, 61–66, 2018.
6. Mira, F., J. Mateu, S. Cogollos, et al., "Design of ultra-wideband substrate integrated waveguide (SIW) filters in zigzag topology," *IEEE Microwave and Wireless Components Letters*, Vol. 19, No. 5, 281–283, 2009.
7. Li, J., C. Ding, F. Wei, et al., "Compact UWB BPF with notch band based on SW-HMSIW," *Electronics Letters*, Vol. 51, No. 17, 1338–1339, 2015.
8. Qiang, L., Y.-J. Zhao, Q. Sun, W. Zhao, and B. Liu, "A compact UWB HMSIW bandpass filter based on complementary split-ring resonators," *Progress In Electromagnetics Research C*, Vol. 11, 237–243, 2009.
9. Ammari, H., M. L. Riabi, F. Grine, et al., "Novel multi-mode wideband filters based on cone half-mode substrate integrated waveguide," *2018 IEEE MTT-S International Conference on Numerical Electromagnetic and Multiphysics Modeling and Optimization (NEMO)*, 1–3, IEEE, 2018.
10. Borazjani, O., M. Nosrati, and M. Daneshmand, "A novel triple notch-bands ultra wideband bandpass filters using parallel multimode resonators and CSRRs," *International Journal of RF and Microwave Computer Aided Engineering*, Vol. 24, No. 3, 2014.